Turbulent Boundary-Layer Growth over a Longitudinally Curved Surface

R. N. Meroney*
Colorado State University, Fort Collins, Colo.

and

P. Bradshaw†
Imperial College of Science and Technology, London, England

Measurements are reported for turbulent boundary-layer growth in a prolonged bend where the additional rates of strain produced by streamline curvature influence the turbulent development. The growth rate of the boundary-layer thickness over the convex side is almost halved and the skin friction coefficient falls to about 0.9 of the value expected on a plane surface. The mixing rate on the concave side is increased to about 1.1 times the plane surface value, and the customary evidence of longitudinal rolls appears. These measurements are the first since those of Schmidbauer's (1936) to provide a test of existing curvature correction formulas for curvatures typical of airfoils and turbomachinery without the complications of compressibility. Results have been compared against calculation techniques proposed by Bradshaw (1973), with good agreement.

Nomenclature

H = shape factor, δ^*/θ
k = curvature parameter, $1/R$
p = pressure
R = radius of curvature
u' = velocity fluctuation
u = mean velocity
u^+ = dimensionless velocity, u/u_τ
v' = velocity fluctuation in vertical
w' = velocity flunctuation in lateral
x = coordinate
y = coordinates
z = coordinate
y^+ = dimensionless vertical coordinate, $u_\tau y/\nu$
β = empirical constant in Bradshaw's curvature correction expression
δ = displacement thickness
θ = momentum thickness
κ = Von Karman's constant
λ = vortex lateral wavelength
ν = kinematic viscosity
ν_τ = turbulent eddy diffusivity
ρ = density

Subscripts and Superscripts

pw = potential value at wall
p = potential core value
ref = reference value
t = total pressure value
sw = static wall pressure value

Received June 20, 1974; revision received November 11, 1974. Work completed at Imperial College of Science and Technology during academic leave from Colorado State University and tenure of a Clean Air Act Fellowship, Enviromental Protection Agency, 1972-1973. Partial support under MoD (PE) Agreement AT/2037/0102 and Office of Naval Research Contract N00014-68-A-0493-0001, Project NR 062-414/6-6-68 (Code 438) is also acknowledged.

Index category: Boundary Layers and Convective Heat Transfer-Turbulent.

*Associate Professor, Fluid Dynamics and Diffusion Laboratory, Civil Engineering Department. Member AIAA.

†Reader, Department of Aeronautics.

Introduction

THE motivation for the present work stems from the observation that streamline curvature in the plane of the mean shear produces surprisingly large changes in the turbulence structure of shear layers. These changes may be more important in magnitude than normal pressure gradients, property variations, or other explicit effects in the mean motion and the turbulence correlation equations for curved flows. Turbulence may be nearly eliminated in some regions of highly convex surfaces, whereas for highly concave surfaces quasi-steady longitudinal vortices may develop to dominate local transport.

We were particularly interested in the penetrative convective instabilities and three-dimensional motions resulting from the action of centrifugal buoyancy forces over concave surfaces. These instabilities are found to take the form of quasi-steady three-dimensional vortices oriented in the streamwise direction. The occurrence of a closely analogous phenomenon in the atmosphere is fairly well documented.[1-3] The large-scale cloud streets frequently observed in satellite photographs are now accepted as direct evidence of the presence of longitudinal vortex instabilities in the earth's atmosphere. the presence of these rolls may well explain the inadequacies of K-theory-type approaches to predict uniformly momentum, heat, or vapor transport through the Earth's boundary layer.

In the atmosphere, these instabilities may be a combination of movements associated with surface heating, curvature, Coriolis forces, and wind shear.[4] Interest in this problem has led us to examine various aspects of the simplified linear and laminar problem, the effects of longitudinal vorticity on heat and mass transport, and the effects of curvature on a turbulent eddy diffusivity model.[5-10] This paper examines directly the influence of such secondary motions on the character of turbulence and transport in well-developed turbulent boundary layers.

An extensive and thorough review by P. Bradshaw[11] now exists. Since this monograph reviews the work on boundary-layer development over two-dimensional curved surfaces from its first presentation in 1930 until the present, only the pertinent conclusions need be presented here. Literature

dealing with the development of longitudinal vortices in the presence of a boundary layer are discussed in more detail in Ref. 26.

One concludes that a full survey of the turbulent system in the presence of developing vortices has not been obtained. No spectra are available, no third-order correlations. Wall shear measurements are limited. Since previous airfoil measurements were limited to velocity profiles and $\delta/R<0.01$ and most channel boundary-layer measurements exceed $\delta/R=0.05$ or 0.1 this study has examined the moderate growth condition where $\delta/R\sim 0.01$-0.02. Turbulent measurements were made to establish flow history, eddy scales, and vortex spacing. Numerically, the value of Bradshaw's length scale modification for curved flows has been examined by use of the Bradshaw, Ferris, and Atwell program.[15]

The test section developed for this study was added to an existing centrifugal fan blower tunnel present in the aeronautical laboratory at Imperical college of Science and Technology. A 10,000-cfm centrifugal fan and a 12.5-kw motor force air through five screens into a plenum chamber. A nine to one contraction ratio reduces the flowfield to a 5×30 in. section with a turbulence level of about 0.1%. The boundary layers develop naturally over a 4 ft 9 in. length before entering the curved section. Boundary-layer thicknesses on top and bottom of the duct are both approximately one inch.

The curved test section is a 5×30-in. extension section 4 ft long with a radius of curvature of 100 in. on the convex side. Static pressure taps are distributed over the section length on both the concave and convex sides. Five 3.5-in. diameter ports are available along the test section centerline. These ports provide access to the flow cross section. When a traversing device is mounted over the port openings, vertical movement over the 5-in. tunnel width is possible and lateral movement over 3 in. is available. A series of stagnation and surface tubes and single- and cross-wire anemometers were attached to the traversing gear.

Twenty-six static pressure holes were distributed over the upper (concave) and lower (convex) sides of the test section. These pressures were normalized by the total head presented by the reference velocity found at the entrance to the 5×30-in. sections. Each surface tap was a $\sim$0.02-in. diameter hole through a brass or plastic insert. All tapes were sanded smooth and checked for burrs or irregularities. Pressure measurements were made by an Airflow Mk 5 inclined manometer.

Two sets of stagnation and surface probes were prepared to measure pressure variation across the wind-tunnel section. When possible, measurements were made along section radii of curvature. The stagnation tubes were constructed from a set of telescoping hypodermic-size stainless-steel tubing and soldered. The tip diameter was flattened to give an elliptic probe 0.025 in. high by 0.055 in. wide. Surface turbes were similarly formed; however, the tips were not flattened. Typical i.d. and o.d. diameters were 0.025 in. and 0.042 in. respectively. Distances of the probes from the wall were determined by a precalibrated traverse potentiometer. Wall location was determined for each measurement by means of a continuity circuit between the probe tip and a thin layer of conductive silver paint applied to the local wall surface.

The hot-wire measurements were all based on the DISA range of equipment. Type 55D01 anemometers and signal conditioning equipment were used. All signals were linearized by the DSIA 55D10 linearizer and DISA 55D25 auxiliary unit, mean signals were measured with the DISA 55D30 digital voltmeter. A DISA 55D26 sum and difference device was utilized to evaluate a set of the cross-wire output voltages. Anemometer output from the X-wire anemometer was recorded on separate channels of an Ampex FR1300 FM analog-type recorder.

Subsequently, analog tapes were digitized by means of a Digital Equipment Co., Ltd. system utilizing an DEC AD-08-B A-to-D converter, a PDP 8/L minicomputer, and an Ampex TM-16 tape transport. The equipment and procedures utilized are described by Brandt and Bradshaw.[16] Digitized signals were evaluated by a program prepared by Dr. C. W. Von Atta and modified for used on the CDC 6400 system at Imperial College by Antonia and Bradshaw.[17]

Measurement Techniques and Data Reduction Procedures

A conventional pitot-static probe is not appropriate for flow following curved streamlines because of the significant vertical static pressure gradient. Hence, only stagnation tube measurements were made across the tunnel section. Fortunately, given the radius of curvature of the flow, one can determine the local static pressure from its value at the wall or one can integrate the stagnation pressure results outward from the wall.[12,18] Both methods were used to calculate local longitudinal velocity; however, the latter method seemed showwhat inconsistent, perhaps because of the accuracy required by the numerical integration. The expression utilized for the results displayed herein was

$$u/u_{pw}=[(p_t-p_r/p_r-p_{sw})+e^{-2ky}]^{1/2} \tag{1}$$

where $u_{pw}=(2\ (p_r-p_{sw}))^{1/2}$; $p_r=$ reference total pressure in potential core region; $p_t=$ local total pressure; $p_{sw}=$ static pressure at wall; and $k=1/$radius of curvature.

This expression is obtained from the Bernoulli equation under the assumption $\partial p/\partial y=k\rho\ u^2$. Small terms which represent the difference between the static pressure calculated from the actual velocity and the potential velocity are dropped in this approximation. The major source of errors of a total-head probe are the effect of turbulence, the effect of yawing, and the effect of wall. The errors due to the effects of turbulence are not well understood; various authors have suggested corrections ranging from positive to negative value for the same condition. However, for turbulence less than 10%, the error in total pressure is probably less than 1% of the dynamic pressure. Total-head tubes are rather insensitive to yaw, misalignments of $\pm 15°$ are required to produce errors of order of 1%. Corrections for the wall effect are made using the curve of Stanton et al.,[19] however, these should be significant only for the closest to the wall measurements.

Some care must be taken in defining the integral boundary-layer parameters for a curved flowfield. Since the potential velocity distribution increases linearly across the duct it is inappropriate to define a boundary-layer thickness as 99% of some specific velocity value. Rather, all velocities in the boundary layer should be compared with the potential velocity which would exist for an inviscid fluid; therefore, to be consistent the momentum and displacement thicknesses are defined as

$$\theta=\int_0^\infty \frac{u(y)}{u_p(y)}\left[1-\frac{u(y)}{u_p(y)}\right]dy \tag{2}$$

$$\delta^*=\int_0^\infty\left[1-\frac{u(y)}{u_p(y)}\right]dy \tag{3}$$

$$H=\delta^*/\theta \tag{4}$$

Surface or Preston tube measurements were evaluated by arguing the pressure difference Δp between the stagnation tube resting on the surface and a nearby static-pressure tap should be only a function of shear stress τ_w, the tube diameter d, and the properties of the fluid ρ, and ν. We thus obtain

$$\Delta p\ d^2/\rho\ \nu^2=f_1(\tau_w\ d^2/\rho\ \nu^2) \tag{5}$$

or rearranging

$$\tau_w/\Delta p=f_2(\Delta p\ d^2/\rho\nu^2) \tag{6}$$

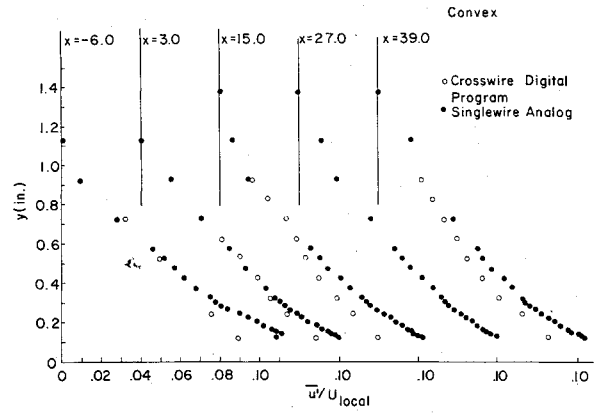

Fig. 1 Longitudinal turbulence intensity over convex wall.

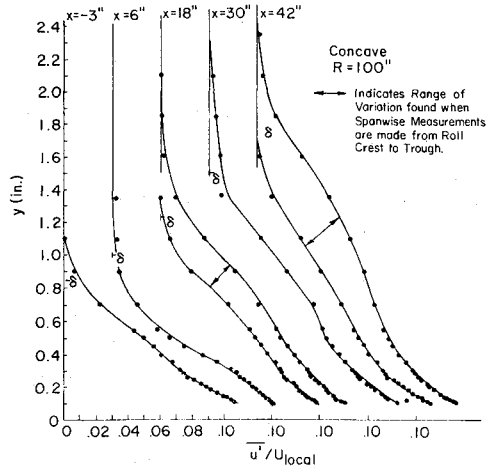

Fig. 2 Longitudinal turbulent intensity over concave wall.

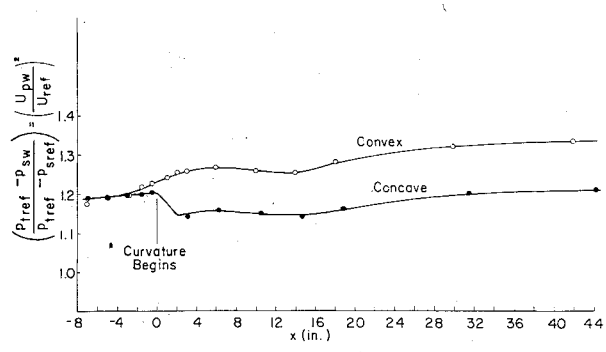

Fig. 3 Wall static pressure distribution.

A calibration chart prepared by F. Wong (Imperial College Aeronautic Notes for Undergraduates) from the measurements of V. C. Patel was used to interpret the measurements.[20]

A second measurement of local skin friction was obtained by the classical Clauser chart technique. This technique assumes the presence of a universal logarithm velocity law near the wall. This law must be modified, however, to reflect the presence of mild curvature effects. An appropriate universal expression with mild curvature is[21]

$$u = (u_\tau/\kappa)\,(\ell n(u_\tau y/\nu) + (2\beta/\kappa)\int u\,dy) \qquad (7)$$

or for $U \alpha y^{1/5}$ in the inner layer

$$u[\,(1-2\cdot(5/6)\beta(y/R)\,[= (u_\tau/\kappa)\,(\ell n(u_\tau y/\nu) + kC)\,] \qquad (8)$$

Therefore one may plot

$$(u/u_{pw})\,[1-(5/3)\beta(y/R)\,]\text{vs}\ u_{pw}y/\nu \qquad (9)$$

for various values of u_τ. (u_{pw} is potential velocity which would exist at wall for an inviscid flow). See Figs. 1 and 2 for results over convex and concave surfaces. So and Mellor were pessimistic concerning the presence of a logarithm region over a concave surface.[12] However, the results found herein appear consistent.

Mean temperature of the flowfield was monitored throughout the experiment by a thermistor probe. This was especially critical because of the thermal drift which occurred daily in the laboratory. Runs where temperature drifted by more than 5°F were discarded.

The hot-wire anemometer was only used to determine fluctuating quantities in the process of these experiments. Every effort was made to eliminate the effects of temperature drift by taking a data set promptly and measuring primarily dimensionless quantities. Single- and cross-wire anemometer systems were used to measure fluctuating quantities. Voltages were evaluated in the conventional manner by an analog system.[16,23,24] As an additional check on accuracy and to obtain higher order correlations the cross wire signals were analyzed digitally. The techniques described by Castro[24] and Brandt and Bradshaw[16] were followed. Whether results are analog or digital are so noted on the figures.

Results and Discussion

In the following, the discussion is divided into three sections. The first deals with efforts to check the "well behaved" nature of the flow, i.e., presence of separation or secondary flow. The second deals with the convex-flow results and the third the concave results. The discussion takes the following format. The mean-flow data are analyzed first, followed by a discussion of the turbulence data.

General Flowfield

Uniformity and straightness of flow in the curved section was checked by observing tufts attached to the wall of the tunnel. In addition, smoke was released from a TEM model smoke probe. The flow remained attached and appeared visually uniform. A stethoscope was used to check for turbulence and the extent of the wall region at the duct outlet. The boundary layer was thicker on the top concave surface than on the bottom convex surface. The shear-layer thickness appeared constant with no asymmetry with respect to duct centerline. The potential core region appeared turbulence free. The large aspect ratio of the duct (1:6) apparently helped to avoid large secondary wind veering typical of early experiments in rectangular ducts.

As a further check of the flow symmetry, two ¼-in. diam cylinders were placed normal to the flow, perpendicular to the duct wall surface, and equal distance from the duct centerline (~4 in.). The wakes produced by these cylinders were examined at the duct outlet. There was no evidence that the wake profiles were deflected to either side over the length of the test section.

The pressure distributions the length of the entrance and curved wall sections are shown in Fig. 3. The cross-duct pressure distribution appears to adjust and balance for the curvature within two duct heights (~10 in.). This sudden pressure adjustment cannot be eliminated since it is inherently characteristic of a change from a straight to a curved flowfield. Even so the total maximum pressure change amounts to less than 10% of the reference dynamic head. Since the curvature was relatively mild and the duct aspect ratio rather large, no wall jets or flaps were employed to tailor the pressure distribution. It was felt that the effects of mild pressure variation are well understood and can be corrected for in any current numerical boundary-layer calculation method.

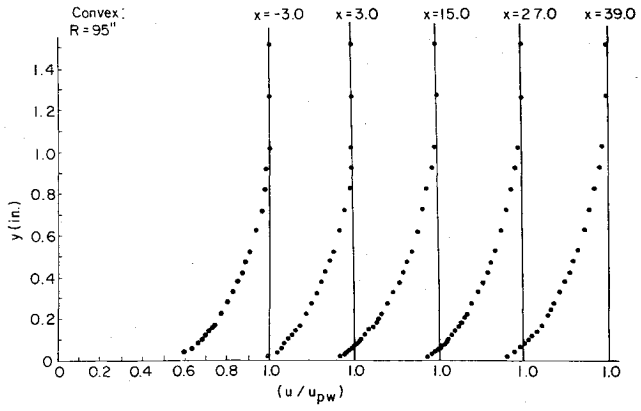

Fig. 4 Velocity profiles over convex wall.

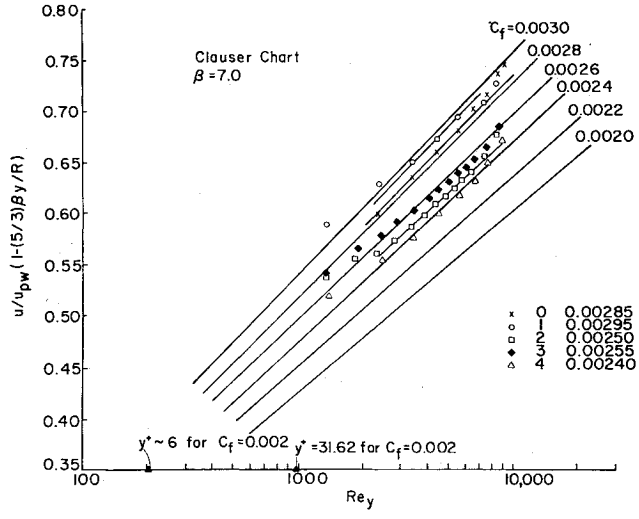

Fig. 5 Modified Clauser chart: convex wall.

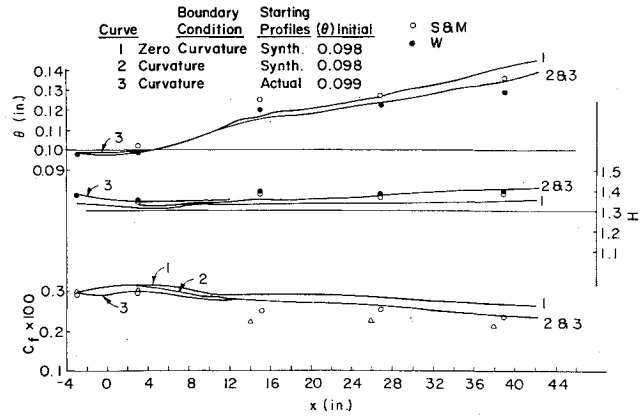

Fig. 6 Variation of integral boundary layer characteristics over convex wall.

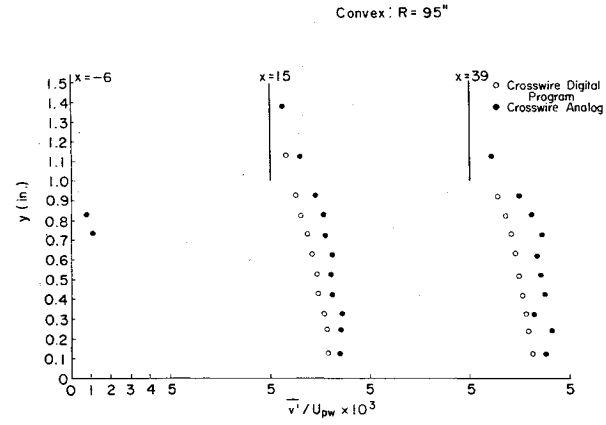

Fig. 7 Vertical turbulent intensity over convex wall.

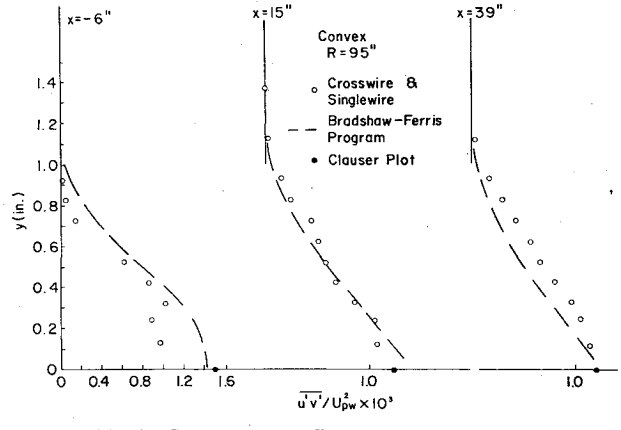

Fig. 8 Shear stress profile over convex wall.

Convex Surface Effects

The sequence of mean velocity profiles which grow over the convex side are shown in Fig. 4. Note the low rate of boundary-layer growth, which is almost half what would be expected for the corresponding straight section. The profile gradients become less intense near the wall and the power law parameter increases from 1/7 toward 1/2. Since the skin friction is not measured independent of the velocity profile, the skin friction quoted depends on the validity of the modified Clauser plot or the Preston tube to determine C_f for curved flow. The measured velocity profiles were plotted in Clauser plot form in Fig. 5. All profiles show an extensive straight-line region which begins to deviate at the same point ($yu_\tau/\nu \approx 200$) where a flat-plate profile begins to deviate from the Law of the Wall. Thus, it can be said that a modified Law of the Wall, which is given by $u^+[1-(5/3)\beta(y/R)] = (1/\kappa)(\ell n)y^+ C$ exists for flow along convex surfaces.

For flows over convex surfaces, the centrifugal force on a fluid element must be balanced by an inward pressure gradient. If a particle is moving too fast (or slow) for its location, the centrifugal force component is large (or small), and the particle moves outward (or inward). Hence, in a turbulent flow the vertical motions over a convex surface are hindered, resulting in a decrease in the interchange of momentum and energy.

Consider Fig. 6 which displays the variation of skin friction C_f, momentum thickness θ and a shape factor H over the span of the convex wall. A curvature perturbation of $\delta/R \simeq 0.01$, which might be expected to cause only a 1% change in the Reynolds' stress equations, has resulted in approximately a 10% decrease in skin friction, a decreased rate of momentum thickness growth and a slight increase in shape factor. Also included in Fig. 6 are lines depicting behavior as predicted by the hyperbolic boundary-layer program of Ferris and Bradshaw,[25] modified for a curvature correction as described by Bradshaw.[13,14] For a constant β of 7.0 the results display fairly good agreement with the experimental data.

The decrease in mixing activity is also evident from the turbulence measurements, Figs. 1, 7, 8. It can be seen that there are significant decreases in the turbulent intensities across the boundary layer.

The change in the $\overline{u'v'}$ profile from that corresponding to flat-plate flow is especially interesting. Most of the suppression occurs in the outer region of the boundary layer. Extrapolated values of the shear near the wall closely approximate the results from the Preston tube of the Clauser plot. The flow perceives a favorable pressure gradient initially as it readjusts to curved flow lines; subsequently, the convex

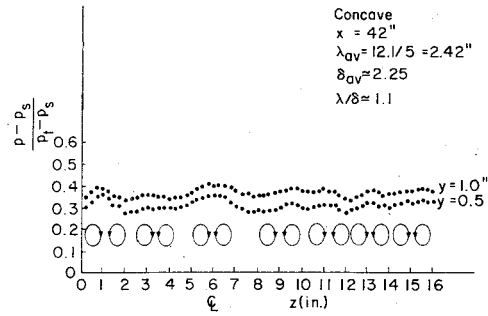

Fig. 9 Lateral stagnation pressure traverse at duct exit over concave wall.

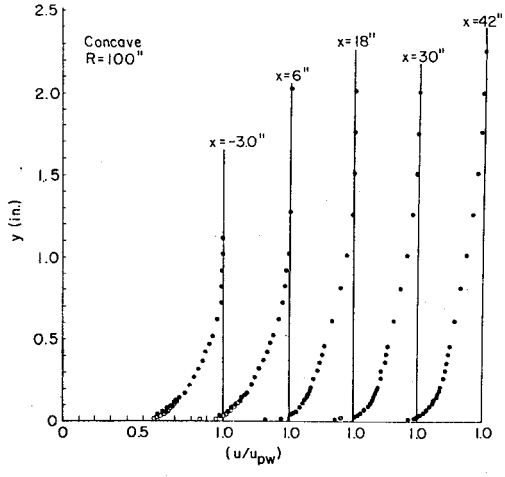

Fig. 10 Velocity profiles over concave wall.

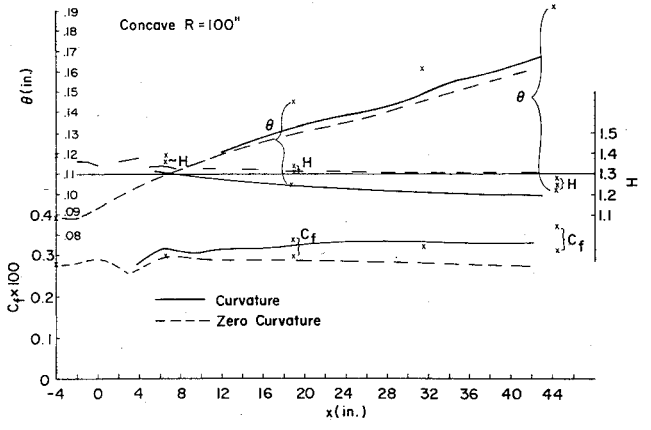

Fig. 11 Variation of integral boundary layer characteristics over concave wall.

curvature prevents the turbulence intensity from increasing. Examination of the intensities $\overline{u'v'}$ and the shear $\overline{u'v'}$ suggests the flow has almost reached a new equilibrium state where profiles become similar.

Concave Surface Effects

The distinguishing characteristic of flow over the concave surface is the presence of significant lateral variation in all flow properties. A survey of stagnation pressure at two heights (1.0 and 0.5 in.) above the surface over a 16-in. lateral fetch is shown in Fig. 9. The pressure variations can be explained by assuming the existence of a system of longitudinal vortices similar to the Taylor-Gortler-type vortices inside the boundary layer. The positions of the high points (crests) on the trace can be taken to correspond to the position between two vortices whose flow direction is toward the wall, and the position of the low points (trough) could be taken as a position between the vortices where the flow directions are

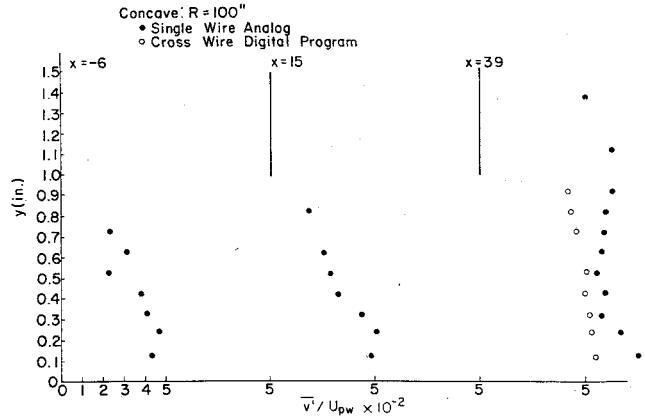

Fig. 12 Vertical turbulent intensity over concave wall.

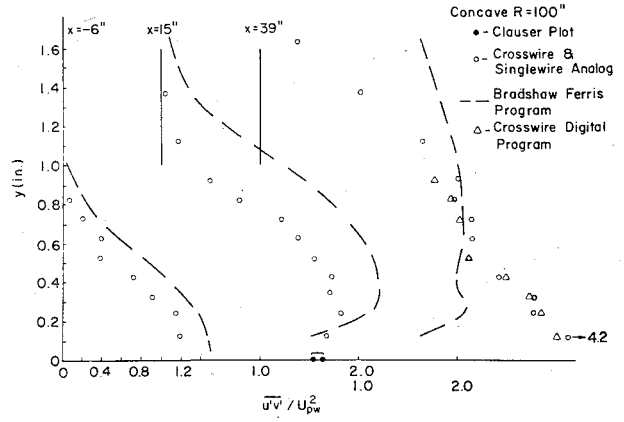

Fig. 13 Turbulent shear stress profile over concave wall.

away from the wall; thus, the wave-like behavior. The boundary-layer thickness at this position was of the order of 2-2½ in. the apparent wavelength between rolls was approximately 2.42 in. These rolls and their positions were very stable. Traverses made at two different times some days apart reproduced the same structure. It is probable that the exact roll positions are tied in some manner to irregularities in upstream screens, boundaries, or turbulence transition location.

The growth of the mean velocity distribution along the concave surface and down the centerline of the duct is shown in Fig. 10. Boundary-layer thickness varies by 25% over the wavelength of each roll. Momentum thickness varies from 50 to 100% over a roll width. Local skin friction appears to vary by 20%. All of this arises from only a magnitude of $\delta/R \cong 0.02$.

The test span variation of C_f, θ, and H are shown in Fig. 11. Again one sees the influence of curvature; however, this time centrifugal effects act to enhance mixing and increase momentum transport on the average. A two-dimensional analysis will obviously be unable to predict the nature of the three-dimensional influence of longitudinal rolls. Nonetheless, the predictive results of the method of Bradshaw are displayed as before. An average 10-12% increase in skin friction, a decrease in shape factor, and an increase in momentum thickness are suggested. The experimental variation in C_f and H are not nearly so great as the variation in θ.

To interpret the hot-wire anemometer results one must assume that the lateral velocities developed by the roll do not significantly change the signal measured. With this rather serious limitation in mind one can examine Figs. 2, 12, 13.

Profiles of $\overline{u'}/u$ are shown in Figs. 2. At stations $x=3$ in,6 in., and 30 in. measurements were taken at the duct centerline. However, at $x=18$ in. and 42 in. spanwise measurements were also made. The curves identified by arrows on the figure bracket the variation across a longitudinal roll. The rapid

penetration of turbulent energy into the potential core region, together with a significant spanwise variation is apparent. Figure 12 displays a similar behavior for $\overline{v'}/u_{pw}$; however, the character of $\overline{u'v'}/u_{pw}$ is perhaps most interesting.[2] In a flat-plate boundary layer the constant flux region extends outward to 0.15 δ. For this concave boundary-layer case the results suggest a nearly constant shear extending to 0.3-0.45 δ.

Conclusions

As a result of this investigation a body of data was developed on boundary-layer flow over moderately curved convex and concave surfaces. The following conclusions may be drawn from examination of the results and comparison with recent analytical models.

Turbulent Boundary Layers along Convex Surfaces

a) The Law of the Wall holds in a modified form along covex surfaces.

b) Initial and subsequent decreases in the intensities of turbulence are due, partly to favorable pressure gradient and, partly to curvature. The curved streamlines interact with the boundary layer to inhibit vertical mixing.

c) The shear stress decreases steeply outside the near wall region and approaches zero well inside the typical boundary layer (about 0.88 for $\delta/R \simeq 0.01$).

d) A length scale correction of the sort proposed by Bradshaw suffices to predict the effect of moderate convex curvature in skin friction, shape factor, and momentum thickness.

e) A small change in curvature ($\delta/R \simeq 0.01$) arouses a large (10%) change in integral properties of the flowfield.

Turbulent Boundary Layers along Concave Surfaces

a) The Law of the Wall appears to hold in a modified form along concave surfaces when the spanwise local friction velocity is used as the velocity scale.

b) Concave curvature may induce parallel sets of longitudinal rolls in the turbulent boundary layer. These rolls appear to extend the height of the boundary layer and characteristically show a wavelength of the order of the boundary-layer thickness.

c) As a result of increased mixing promoted by the concave curvature, there is a substantial increase in the turbulent energy all across the boundary layer.

d) The various turbulence correlations and mean velocities are distributed laterally in a wave-like manner, indicating the presence of a vortex system.

e) The shear correlation coefficient appears to remain large for an extended distance from the wall before it begins to diminish. Detailed tabulated data and further measurements for the experiment are available in the report described as Ref. 26.

References

[1] Kuettner, J., "The Band Structure of the Atmosphere," *Tellus*, Vol. 11, 1959, pp. 267-294.

[2] Kuo, H. L., "Perturbations of Plane Couette Flow in Stratified Fluid and Origin of Cloud Streets," *Physics of Fluids*, Vol. 5, 1963, pp. 195-211.

[3] Scorer, R., *Clouds of the World*, David and Charles Ltd., 1972.

[4] Faller, A. J., "Large Eddies in the Atmospheric Boundary Layer and Their Possible Role in the Formation of Cloud Rows," *Journal of Atmospheric Sciences*, Vol. 22, March 1965, pp. 176-184.

[5] Rayt, M. J., "Longitudinal Rolls in Layers of Water," AIAA Paper 73-42, Washington, D. C., 1973.

[6] Kahawita, R. A. and Meroney, R. N., "The Influence of Heating on the Stability of Laminar Boundary Layers Along Concave Heated Walls," Submitted to *Journal of Applied Mechanics*, CEP 72-73 RK-RNM79, ASME, 1974.

[7] Kahawita, R. A. and Meroney, R. N., "Convective Instabilities in Parallel, Quasi-Parallel, and Stationary Flows," Rept. CER 73-74 RK-RNM-12, Sept. 1973, Fluid Dynamics and Diffusion Lab., Colorado State University, Colo.

[8] Kahawita, R. A. and Meroney, R. N., "The Vortex Mode of Instability in Natural Convection Along Inclined Plates," *International Journal of Heat and Mass Transfer*, Vol. 17, 1974, pp. 541-548.

[9] Meroney, R. N. and Hsi, G., "Vortex Enhancement of Parallel Plate Plate Heat and Mass Transport," Paper CEP 71-72 Fluid Dynamics and Diffusion Lab., Colorado State University, Colo. RNM-GH-38.

[10] Anyiwo, J. C. and Meroney, R. N., "Effective Viscosity Model for Turbulent Wall Boundary Layers," *Aeronautical Quarterly*, Vol. 24, May 1973, pp. 92-102.

[11] Bradshaw, P., "Effects of Streamline Curvature on Turbulent Flow," NATO, AGARDmonograph No. 169, Aug. 1973.

[12] So, R. M. and Mellor, G. L., "An Experimental Investigation of Turbulent Boundary Layers Along Curved Surfaces," NASA CR-1940, April 1972.

[13] Bradshaw, P., "The Analogy Between Streamline Curvature and Buoyancy in Turbulent Shear Flow," *Journal of Fluid Mechanics*, Vol. 36, Part 1, March 1969, pp. 177-191.

[14] Rastogi, A. K. and Whitelaw, J. H., "A Procedure for Predicting the Influence of Longitudinal Curvature on Boundary Layer Flows," Imperial College of Science and Technology, Rept. of Mechanical Engineering Tech. Report BL/TN/A37, 1974.

[15] Bradshaw, P., Ferris, D. H. and Atwell, N. P., "Calculation of Boundary Layer Development Using the Turbulent Energy Equation. NPL Aero Report 1182, 1966 and *Journal of Fluid Mechanics*, Vol. 28, Part 3, May 1967, pp. 593-616.

[16] Brandt, A. and Bradshaw, P., "Apparatus and Programs for Digital Analysis of Fluctuating Quantities in Turbulent Flow," Dept. of NPL Aero Report 1269, National Physical Lab., Teddington, England, March 1968.

[17] Antonia, R. A. and Bradshaw, P., "Conditional Sampling of Turbulent Shear Flows," Imperial College Aero Rept. 71-04, London, 1971.

[18] Wilcken, H., "Effect of Curved Surfaces on Turbulent Boundary Layers," NASA TT F-11421, 1967, (translation of "Turbulente Grenschichten ar Gewoelbten Ebechen," Eng. Arch., Vol. 1, 1930.

[19] Stanton, T. E., Marshall, D. and Bryant, C. N., "On the Conditions at the Boundary of a Fluid in Turbulent Motion," *(Proceedings Royal Society of London)*, Series A, No. 97, 1920.

[20] Patel, V C., "Calibration of the Preston Tube and Its Limitations on its Use in Pressure Gradients," *Journal of Fluid Mechanics*, Vol. 23, Part 1, Sept. 1965, pp. 185-208.

[21] Bradshaw, P., "Advances in Turbulent Shear Flow," Notes for von Karman Institute for Fluid Dynamics Short Course, March 19-23, 1973.

[22] Bradshaw, P., *An Introduction to Turbulence and Its Measurement*, Pergamon Press, Oxford, 1972.

[23] Sandborn, V. A., *Resistance Temperature Transducers*, Meteorology Press, Fort Collings, Colo., 1972.

[24] Castro, I. P., "Digital and Analog Reduction of Basic Hot Wire Data," Dept. of Aeronautics, Imperial College of Science and Technology, London Notes, Jan. 1972.

[25] Ferris, D. H. and Bradshaw, P., "A Computer Program for the Calculation of Boundary Layer Development Using the Turbulent Energy Equation," NPL Aero Report 1269, National Physical Lab., Teddington, England, March 1968.

[26] Meroney, R. N., "Measurements of Turbulent Boundary Layer Growth Over a Longitudinally Curved Surface," Project Themis Technical Rept. No. 25, Fluid Dynamics and Diffusion Lab., Colorado State University, Fort Collings, (CER73-74RNM26), 1974, (also as Imperial College Aeronautics Rept. 74-05-Jan. 1974, London).